Massive Machine Type Communication using Non-Orthogonal Multiple Access with Convolutional Neural Network Approach

Veronica Windha Mahyastuty, Iskandar, Hendrawan and Mohammad Sigit Arifianto

School of Electrical Engineering and Informatics
Institut Teknologi Bandung
Bandung, Indonesia
windha@students.itb,ac,id, iskandar@stei.itb.ac.id, hend@stei.itb.ac.id,
msarif2a@stei.itb.ac.id

Abstract: The 5G cellular network supports massive Machine Type Communication (mMTC) for Wireless Sensor Network (WSN) application. In this paper, High Altitude Platforms (HAPs) is used as a replacement for Base Station (BS). So that the cluster head (CH) from every cluster will send information owned to the HAPs by using the Power Domain Non-Orthogonal Multiple Access (PD NOMA) as a multiple access technique. PD NOMA uses the Successive Interference Cancellation (SIC) technique on the receiver side. SIC process is proven effective for detecting PD NOMA signal by sorting the received signal strength and then decoding it. However, error from the prioritized signal that has high decoding has a tremendous impact on the prioritized signal that has a way lower decoding, and this error can then further spread with the SIC process. In this paper, we propose a Convolutional Neural Network (CNN) approach to decode information from multiple CH without performing traditional communication signal processing. The simulation is already done by the Rician channel with 11 CH that is connected to the HAP. From the series of simulations that have been done, we can see that the CNN used to replace the conventional SIC on the uplink PD NOMA can detect NOMA signals without the use of conventional signal processing. The CH node nearest to the HAP requires a lower SNR than the CH node farthest from the HAP to achieve BER = 10-4 in both conventional uplink PD NOMA and uplink PD NOMA with CNN. Uplink PD NOMA with CNN has a lower complexity than conventional uplink PD NOMA.

Keywords: *cluster head, HAP, NOMA, SIC, CNN*

1. Introduction

The 5G cellular network supports massive Machine Type Communication (mMTC) for Wireless Sensor Network (WSN) application. In this paper, High Altitude Platforms (HAPs) is used as a replacement for Base Station (BS). So that the cluster head (CH) from every cluster will send information owned by the HAPs by using the Non-Orthogonal Multiple Access (NOMA) as a multiple access technique.

NOMA has the potential to accommodate massive connectivity and increase the system throughput, enabling users to share the same resource, whether in time, frequency, or code through power-domain or code-domain multiplexing techniques [1]. NOMA has been investigated to deal with Orthogonal Multiple Access (OMA) problems such as OMA cannot always reach the total capacity of a multiuser wireless system [2] and in conventional OMA schemes, the maximum number of supported users is limited by the total number and breakdown of the orthogonal resource scheduling. NOMA allows for controlled interference with non-orthogonal resource allocation with a tolerable increase in receiver complexity. Compared to OMA, NOMA's main advantages are increasing spectral efficiency, supporting massive connectivity, low transmission latency, and signaling cost. Due to these advantages, NOMA has been actively investigated as a promising technology for 5G [3].

In general, NOMA schemes can be classified into two types: power-domain multiplexing and code-domain multiplexing. In power-domain multiplexing, different users are allocated different power coefficients according to their line conditions to achieve high system performance. In particular, some user information signals are superimposed on the transmitter side. On the receiving end, successive interference cancellation (SIC) is applied to decode the

Received: October 27th, 2021. Accepted: March 25th, 2022
DOI: 10.15676/ijeei.2022.14.1.8

trade-off between system throughput and user fairness. In code-domain multiplexing, different users are allocated different codes and are multiplexed through the same time-frequency resources, such as multiuser shared access (MUSA) [5], sparse code multiple access (SCMA) [6], and low-density spreading. (LDS) [7].

Although code-domain multiplexing has the potential to improve spectral efficiency, it requires high transmission bandwidth and is not easy to implement in current systems. On the other hand, power-domain multiplexing has a simple implementation as no significant changes are required to the existing network. In addition, it does not require additional bandwidth to increase the spectral efficiency [8].

Power Domain NOMA uses Successive Interference Cancellation (SIC) on the receiver side. SIC process is proven effective for detecting NOMA signal by sorting the received signal strength and then decoding it [9]. However, error from the prioritized signal that has high decoding has a tremendous impact on the prioritized signal that has a way lower decoding and this error can then further spread with the SIC process.

The investigation of SIC based on deep learning for the usage in the NOMA communication system has been done by [10]. In [10] suggested that SIC based CNN increases the performance of a single base station and multiuser NOMA scheme. The architecture of CNN is the one suggested by [10] that consists of 8 layers. In [10], NOMA simulation for downlink direction on the Rayleigh channel by using the simulation program "python". The number of users that is simulated by [10] are 2 and 4 users, with a coefficient of power allocation for user 1 is 0.1 and 0.3. The simulation done by [10] showed that the SIC method-based CNN succeeded to reduce the imperfections of conventional SIC and achieve great detection performance. As a result, the SIC scheme-based CNN can be assumed a potential technique for NOMA detection usage.

The DenseNOMA system to detect uplink NOMA signal was proposed by [11]. DenseNOMA system is designed to be suitable for characteristics of uplink NOMA signal. The architecture of DenseNoma is designed by [11] that consists of nine layers. In [11], the DenseNOMA system is simulated by using the Python and Matlab simulation. This simulation is conducted in the Rayleigh channel, with a total user of 2, coefficient power allocation for the first user is 0.8, and sink node in a form of a Base Station (BS). In this research, [11] send two different signals and trained the BTS. BTS that is simulated has Machine Learning to clarify the signal that is received. From the series of simulations done by [11], it can be seen that the Deep Learning (DL) method that is proposed can handle the NOMA signal with the carrier immediately without any traditional signal processing. The processing and detecting of signal that is optimal can be done by the DL approach intelligently without any complex modularity receiver design. In [11], did not conduct research for coefficient power allocation for more than two users, so it cannot be proven that CNN can conduct a classification of more than two users. So, we conduct 11 users in this research that send information to sink nodes in the form of HAP with conventional NOMA and NOMA that use CNN.

The Single Carrier-Index Modulation NOMA (SC-IM NOMA) scheme for massive Machine Type Communications (mMTC) was proposed by [12]. This scheme allows users to transmit their data via SC-IM, while massive access is achieved through NOMA. The system model proposed by [12] is for an uplink scenario, where two users transmit their messages to the Base Station (BS). Both users send their SC-IM-based message signals to the BS with powers P_1 and P_2 respectively. Then in the BS, there is a SIC process, where the BS will first recover the signal that has the highest power, namely UE_1 and treats UE_2 as noise. After the BS has successfully recovered the UE_1 signal, the signal will be subtracted from the combined signal. Then, the BS will recover the UE_2 signal. To overcome the shortcomings of the SIC process, [12] uses another detector, namely the Joint Maximum Likelihood (JML). The performance of the technique proposed by [12] was analyzed and compared with conventional SC-NOMA. The performance indicators analyzed by [12] are energy efficiency and Bit Error Rate (BER). From the analysis conducted by [12], it can be seen that SC-IM NOMA provides better performance than conventional SC-NOMA.

Analysis of power allocation for NOMA-based D2D communication has been done by [13]. In [13], a novel algorithm is proposed, in which the downlink result is combined with the D2D mode and utilizes the Greedy Asynchronous Distributed Interference Avoidance Algorithm (GADIA) to create different application scenarios. This algorithm provides a simple fully distributed dynamic frequency allocation strategy, without any information exchange between autonomous system equipment and no knowledge of the existence of autonomous entities. The system model proposed by [13] uses one Base Station (BS) and K cellular users, namely UE_1, UE_2, …, UE_K. Among them, UE1 is closest to the BS with the best channel conditions, and UE_K is at the edge of the cell with the worst channel conditions. In the two-stage NOMA-D2D model, UE2 can act as a relay for UE_1, whereas UE_2 can directly communicate with UE_3 as a D2D transmitter. In the first stage, the BS sends signals to UE_1 and UE_2 in NOMA mode; in the second stage, UE_2 acts as a D2D relay and transmitter and also sends signals to other users in GADIA mode. Research conducted by [13] focuses on downlink scenarios. Then, the model system is simulated using Matlab and numerical evaluation is carried out. In [13], the performance of maximum achievable rate and energy efficiency (EE) at a given spectral efficiency (SE) is compared using either NOMA or Orthogonal Frequency Division Multiple Access (OFDMA). From a series of simulations and numerical evaluations, it can be seen that NOMA has better performance than OFDMA.

Our main contribution is to create a WSN system-based HAP using NOMA as a multiple access technique, in particular as follows:

1. We create a WSN system that consists of 11 nodes as a cluster head (CH) that is connected with HAP. Each CH node will send information sensing to HAP using Power Domain NOMA (PD NOMA) as a multiple access technique. The 11 CH nodes are obtained from our previous research result about clustering [14] with a condition that HAP moves vertical, horizontal, and inclination. The system we made is different from [11], we use 11 users while [11] only uses 2 users. The power allocation that we use is also different from [11].
2. We simulated 11 nodes that are connected to HAP on the Rician channel. This is different from [11] which uses the Rayleigh channel.
3. We replace the SIC process in HAP by using deep learning, especially Convolutional Neural Network (CNN). We adopted the idea [11] of using CNN to replace the SIC process. But the difference is, the sink node that we use is HAP, while [11] uses BS.
4. We compare WSN system performance-based HAP using conventional PD NOMA with the one using PD NOMA with CNN. The performance indicator that we evaluate is Bit Error Rate (BER).

2. Basic Principle of 5G Over HAPs

Technology developments caused changes in the 5G network business. This change is marked by a shift in communication trends toward Machine Type Communication (MTC), whereas tens of billions of smart devices will use embedded communication capabilities and integrated sensors to act in their local environment.

The 5G network supports massive Machine Type Communication (mMTC) applications. mMTC happens in-between machines that have the potential for communication/computation without intervention from a human. The main feature of mMTC is that it generates data automatically, processing, transferring, and switching information in-between machine that is intelligent and intervention that is minimum from human [15]. mMTC connects a large number of devices such as smart metering, sensors, and smart grid equipment over a wide coverage area [16]. One of the mMTC applications is to monitor and sense [17][18]. Monitoring and sensing are modeled with *Wireless Sensor Network* (WSN).

WSN is an intelligent network application system that collects, integrates, and transmissions data autonomously [19]. Sensor nodes are usually spread in the sensor area [20]. Every sensor node that is spread has the potential to collect and route data through the Internet or even satellite. So, the data can be accessed by the user. The main obstacle in using WSN is

the limited power that is owned by each sensor node One of the solutions to cope with it is by using the clustering method.

The sink node on WSN is replaced with a High-Altitude Platform (HAP) in this research. (HAP) is an airship or plane that operates in the stratosphere at the height of 17-22 km. This platform has the potential to send information very fast and can serve a huge number of users using fewer communication infrastructures than terrestrial [21]. HAP system has a few advantages, including easy implementation, flexibility for reconfiguration, low operation cost, low propagation delay, high elevation angle, wide coverage, has the potential to broadcast/multicast as well as broadband and move in an emergency [22].

HAP position in the stratosphere layer is affected by wind and the physical condition of the stratosphere layer. This HAP movement includes [23]:

1. Vertical Movement
   At first, HAP is positioned at "h" altitude from the Earth's ground, then vertical movement as big as Δh happens, so the altitude of HAP now becomes h ± Δh. As a result of this vertical movement, the size of the coverage area of HAP changes, as can be seen in Figure 1.

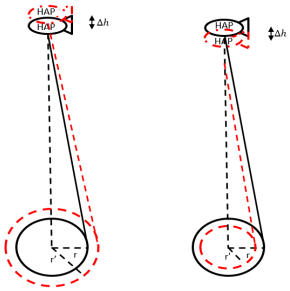

(a). (b).

Figure 1. The change in the size of the coverage area of HAP because of vertical movement, (a) HAP is at the altitude of h + Δh, (b) HAP is at the altitude of h – Δh

2. Horizontal Movement
   HAP moves to the horizontal direction on air, without being accompanied by the change in HAP altitude. In this case, HAP moves as big as Δr, where Δr ≥ 0. The movement of HAP can be seen in Figure 2. From Figure 2, it can be seen that when HAP moves horizontally, the area coverage of HAP will change but the shape of the area coverage of HAP is still a circle.

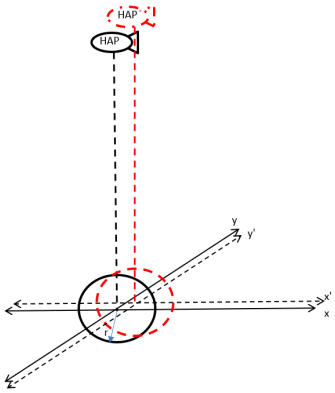

Figure 2. Change in area coverage of HAP because of horizontal movement of HAP

3. Inclination Movement
   HAP on the air rolls or spins according to a certain axis, without being accompanied by the position change of HAP. This movement is called the inclination angle movement of HAP or HAP's tilt [23]. The effect from the inclination movement is relatively much more than the other two movements previously, where the angle of inclination will make the area coverage of HAP on the Earth's ground that initially was a circle-shaped to no longer a circle, the size of the area coverage of HAP can increase and also decrease. Inclination movement of HAP with the initial position of HAP located in the points (0,0), can be seen in Figure 3.

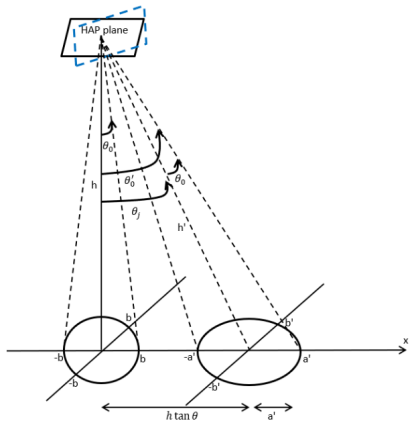

Figure 3. The change in area coverage because inclination movement HAP

From figure 3, it can be seen that the area coverage of HAP that is new is no longer circle shaped, rather an ellipse-shaped.

In WSN over HAP, the cluster head (CH) from every cluster will send information owned by the HAPs by using the Non-Orthogonal Multiple Access (NOMA) as a multiple access technique.

Non-Orthogonal Multiple Access (NOMA) is a multiple access technology that is able to fulfill low latency requirements, high reliability, massive connectivity, and high throughput. Two types of NOMA that are dominant are power domain (PD) and code domain (CD) [2].

PD NOMA allows different users to share time, frequency, and code that is the same, however with different power levels [9]. In PD NOMA, especially uplink PD NOMA, Successive Interference Cancellation (SIC) is used in Base Station. The user is sorted based on the signal strength so the SIC detector first decodes the strongest signal and then subtracts it from the combined received signal and then the second strongest signal can be detected and subtracted from the combined signal, and this process continues - until all signals are detected [9]. Uplink PD NOMA can be seen in Figure 4 [24].

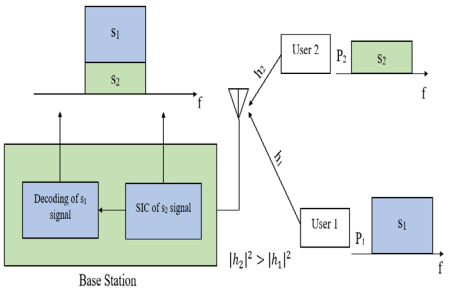

Figure 4. Uplink PD NOMA [24]

The disadvantages of PD NOMA with the SIC process are the complexity of the system which increases with the increase in the number of users and the accumulation of errors during the SIC process [11]. This can be overcome by using machine learning, specifically the Convolutional Neural Network (CNN).

Convolutional Neural Network (CNN) is one type of Deep Learning that attracts the attention of new research. CNN automatically can extract features from the data that is given. The feature obtained is more to representing the data instead of extracting the feature manually that is designed by humans [25].

CNN is used for classifying data that have been labelled using the supervised learning method, where the procedure of the supervised learning is data trained and the targeted variable so that this approach aims to group data inside existing data [26].

CNN is divided based on the data dimension that will be classified. If data is in a form of a 2-dimensional signal (image) then it is called 2D-CNN. Whereas 1D-CNN is used to classify 1-dimensional signals [25]. In this research, we use the 1D-CNN.

3. Research Method

In the previous research [14], clustering for mMTC consisted of 250.000 sensor nodes has been done. In [14], 250,000 sensor nodes are deployed in the HAP coverage area. HAP coverage area for urban areas with a diameter of 63 km coverage area. Then the 250,000 sensor nodes are clustered using the clustering algorithm proposed by [14]. The result of clustering from [14] obtained is 11 clusters. Each cluster has one sensor node that functions as the cluster head (CH). So, in this research, there are 11 CH nodes forward information from each sensor node to the HAP using the NOMA multiple access techniques, specifically the Power Domain NOMA (PD NOMA) with the uplink direction. The network topology of the WSN system with 11 CH nodes connected to the HAP can be seen in figure 5.

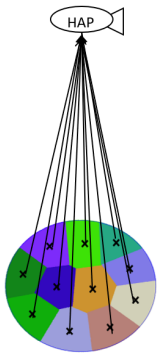

Figure 5. The topology of the WSN system with 11 CH nodes connected to the HAP

In figure 5, the x symbol represents the CH node. From our previous research [5], HAP is located at the altitude of 20 km from the ground's surface and has a diameter coverage area as big as 63 km.

A. Simulation Scenario

The simulation scenario, in this research, is 11 CH nodes that send information to the HAP that uses uplink PD NOMA as a multiple access technique. In this simulation, we use position data of CH nodes when HAP moves downwards vertical by 4 km, rightwards horizontal by 6.5 km, and 10° inclination from the previous research about clustering [14].

In this simulation, the system is compared between using conventional uplink PD NOMA and uplink PD NOMA with CNN. This scenario aims to look at the performance of conventional uplink PD NOMA and uplink PD NOMA with CNN.

A.1.Conventional Uplink PD NOMA

The block diagram from the system that uses conventional uplink PD NOMA can be seen in Figure 6.

From Figure 6, it can be seen there is k CH node, k = 11. Every CH node has information $s_1, s_2, \dots, s_k$ with power allocation $\sqrt{\alpha_1}, \sqrt{\alpha_2}, \dots, \sqrt{\alpha_k}$. α_k is a coefficient power allocation for k-users that can be found by using equation (1).

$$\alpha_k = 0.75 . (0.25)^m, m=0, 1, \dots, k\text{-}1$$

Where α_k is a coefficient power allocation for k-users $\alpha_1 + \alpha_2 + \dots + \alpha_k = 1$ [17–18].

Every CH has 4 transmitter antennas with channel gain from each CH which is $h_1, h_2, \dots, h_k$. Where $h_1 = h_{11}+h_{12}+h_{13}+h_{14}$; $h_2 = h_{21}+h_{22}+h_{23}+h_{24}$; …; $h_k = h_{k1}+h_{k2}+h_{k3}+h_{k4}$.

Path loss between the HAP and sensor node is shown with log-distance path loss and log-normal shadowing model [29]:

$$PL[dB] = FSPL+10\beta log_{10}(d)+X_\delta \quad (2)$$

where *FSPL* is free space loss [dB], β is the path loss exponent, d is the distance between HAP and sensor node [Km]. The value of *FSPL* can be found by using equation (3).

Table 1. Value of β [30]

Environment	Path Loss Exponent
Free space	2
Urban area cellular radio	2.7 – 3.5
Shadowing urban cellular radio	3 – 5
Inside a building - Line of Sight	1.6 – 1.8
Obstructed in building	4 – 6
Obstructed in factory	2 – 3

$$FSPL = 20log_{10}(d)+20log_{10}(f)+32.44 \quad (3)$$

where f is the signal frequency [MHz]. The value of β can be seen in Table 1 [30].

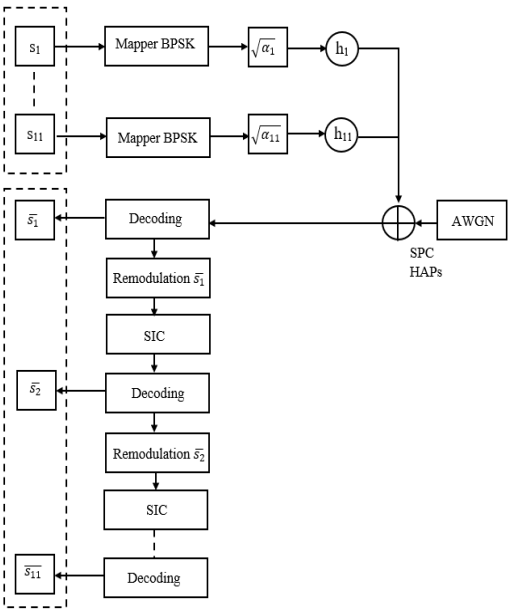

Figure 6. Conventional uplink PD NOMA

Based on Table 1, the value of β is taken as 2. Value of X_δ = 2 dB [29].

In this simulation, we use the Rician distribution as a fading distribution. This is because HAPs' channel distributes Rician. Fading Rician calculates all components Line-of-sight (LOS) and Non-Line-of-sight (NLOS). Probability Density Function (PDF) from Rician distribution [21-23]:

$$f_R(r) = \frac{2(K+1)r}{\Omega} exp\left(-K-\frac{(K+1)r^2}{\Omega}\right) I_0\left(2\sqrt{\frac{K(K+1)}{\Omega}}\, r\right), r\geq 0, K\geq 0, \Omega \geq 0 \quad (4)$$

Value of Ω and K can be found by using equations (5) and (6) [31-32][34].

$$\Omega = E[R^2] = v^2 + 2\sigma^2 \quad (5)$$

$$K = \frac{v^2}{2\sigma^2} \quad (6)$$

Where Ω is the average power, K is the Rician factor, v^2 is the power from the LOS component. $2\sigma^2$ is the power from other multipath components (NLOS) and $I_0(.)$ is the Bessel function order number 0.

In Figure 6, it can be seen that $s_1, s_2, \dots, s_k$ entered BPSK mapper and the process is carried out with equation (7) [35]. The process is done by using ***mod ( )*** function.

$$\bar{s} = \begin{cases} 1, & s=1 \\ -1, & s=0 \end{cases} \quad (7)$$

The output from the BPSK mapper is $\bar{s_1}, \bar{s_2}, \dots, \bar{s_k}$. Then the output from the BPSK mapper is multiplied by power allocation and channel gain. So that the signal that is received by HAP is a superposition coding (SPC) [24]:

$$y = \sum_{i=1}^{k} \bar{s_k} . \sqrt{\alpha_k} . h_k + n \quad (8)$$

Where n is the AWGN noise. With the assumption that $h_1 > h_2 > \dots > h_k$, then the signal that is first decoded is the signal from the first user by doing an equalizer using channel state information (CSI) with the first channel gain value (h_1). The mathematical model for the decoding process uses the ***demod*** $\left(\frac{y}{h}\right)$ function [35]:

$$\hat{s} = \begin{cases} 1, & \left(\frac{y}{h}\right) > 0 \\ 0, & \left(\frac{y}{h}\right) < 0 \end{cases} \quad (9)$$

So that, demodulation on the first user:

$$\widehat{s_1} = demod\left(\frac{y}{h_1}\right) \quad (10)$$

After getting the first estimated user information in the form of bits, the information will go to the process of remodulation, with the function name ***remod( )*** where the function is the same as ***mod( )*** by using equation (7). Besides, the SIC process will be implemented from the first user to the second user, using equation (11) [28].

$$y_{1,2} = y - \left(remod(\widehat{s_1}) . \sqrt{\alpha_1} . h_1\right) \quad (11)$$

After SIC is successfully implemented on $y_{1,2}$, then demodulation will be done for user 2 by using equation (12).

$$\widehat{s_2} = demod\left(\frac{y_{1,2}}{h_2}\right) \quad (12)$$

So that the SIC on user k can be found by using equation (13).

$$y_{k-1,k} = y - \left[\left(remod(\widehat{s_1}) . \sqrt{\alpha_1} . h_1\right) - \cdots - \left(remod(\widehat{s_{k-1}}) . \sqrt{\alpha_{k-1}} . h_{k-1}\right)\right] \quad (13)$$

Demodulation for user k can be found by using equation (14).

$$\widehat{s_k} = demod\left(\frac{y_{k-1,k}}{h_k}\right) \quad (14)$$

A.2. Uplink PD NOMA with CNN

PD NOMA uplink with CNN is PD NOMA uplink that uses machine learning, specifically CNN to replace the SIC process in the receiver. The sending part of the PD NOMA uplink with CNN is the same as the sending part of the conventional PD NOMA uplink. The purpose of replacing the SIC process with CNN is to reduce the complexity of the system and the accumulation of errors that occur during the SIC process. The uplink PD NOMA with CNN can be seen in Figure 7.

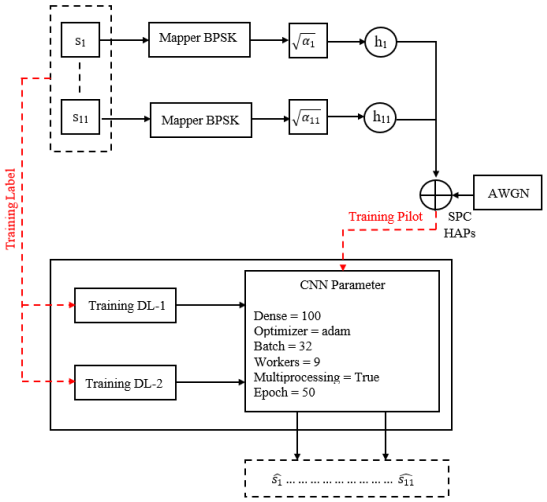

Figure 7. Uplink PD NOMA with CNN

In Figure 7, it can be seen that the SIC process is replaced by CNN. The CNN architecture used in this research can be seen in Figure 8.

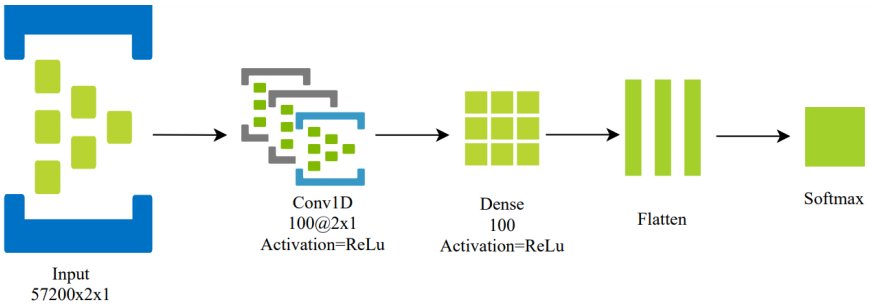

Figure 8. The CNN architecture

In Figure 8, it can be seen that there are five layers from the CNN architecture that is used in the research, which includes the following:

1. Input:
   Input is the matrix input from the dataset that is obtained when BER = 0. The dataset is in the form of a matrix measuring 57200 x 2 x 1. 57200 is the number of bits sent by CH, 2 is its feature, namely the magnitude and angle of the SPC signal received by the HAP.
2. 1 dimension convolutional (conv1D):
   In this CNN architecture, one dimension convolutional is used. This is because the data is a signal of 1 dimension. This layer performs the convolution process from the previous layer's output. In this layer, there are 100 layers with the ReLu activation using two columns of input, which is magnitude and angle from the signal received by HAP.

3. Dense:
   Dense has a function that is the same as convolution but just on a much simple level. Dense is used to connect inter-feature.
4. Flatten:
   Flatten serves to reshape a feature (reshape feature map) into a vector so that we can use it as input from a fully connected layer. The output layers from Dense will be made into one long line or called a concatenate process using flatten ().
5. Softmax:
   Softmax functions to determine user classification based on probability values that have been generated from a series of convolutions on features.

Then input, conv1D, dense, flatten and softmax will be compiled into a CNN architecture system. The optimizer used is "Adam". The loss calculation model used is 'sparse_categorical_crossentropy'. The metric for calculating architectural performance is accuracy.

After the CNN architecture has been successfully made, the next training is implemented as follows:

1. Machine will be given feature input, X which magnitude and angle from the signal that is received by HAP. These features will enter the architecture that has been made.
2. Machine will also be given $Y_{encoder}$ feature filled with label and is obtained from LabelEncoder. In this LabelEncoder, Y, as an example, 0A0A1A1A0A1 (A only as guard bit) is exchanged as a class. So, this input is for the class introduction.
3. After studying, in the training process, testing is carried out using the validation split = 0.1 parameters, meaning that out of thousands of rows, only 10% is taken for validation testing on the machine.
4. In the testing process, 10% of the dataset will give the magnitude and angle of the signal received by the HAP.
5. The machine will issue a Y prediction.
6. After that, the results of the original Y and Y predictions are compared. From as much as 10%, the validation accuracy is checked. The target validation accuracy is 100%.

After training, the next process is as follows:

1. Given SPC signals in the form of magnitude and angle.
2. CNN will issue classes according to the results of the training.
3. From these classes, the LabelDecoder is carried out, which removes the guard bit and returns to the accepted bits for each user.
4. Compare the receive bits with the send bits for each user.

B. Parameter Simulation

Parameter simulation is used in this research which can be seen in Table 2.

Table 2. Parameter Simulation

Parameter	Value
Carrier Frequency	48 GHz
Tx Power	13,4 dBW
Tx Antenna Gain	46 dBi
Number of Tx Antenna	4
Number of Rx Antenna	1
Number of Subcarriers (FFT)	64
Length of Symbol	52
Length CP	16
Total Length	80

Parameter	Value
Modulation Type	BPSK
Dense	100
Optimizer	Adam
Batch	32
Workers	9
Epoch	50

C. Performance Indicator Simulation

The performance indicator that is analyzed in this research is Bit Error Rate (BER).

D. Complexity of conventional and CNN Uplink PD NOMA

Conventional and CNN uplink PD NOMA were analyzed for complexity using Big O Notation.

4. Result and Discussion

A. Conventional Uplink PD NOMA

The results of the BER simulation for the HAP-based WSN system using conventional PD NOMA uplink as a multiple access technique can be seen in Figures 8, 9, and 10.

In Figure 8, it can be seen that to reach BER = 10^{-4}, CH 1 (u1) node needs SNR = 35 dB. Meanwhile, CH 11 (u11) node needs SNR = 105 dB. This shows that CH 1 node requires the smallest SNR to reach BER = 10^{-4} compared to CH 11 node. The difference in SNR between the CH 1 node and the CH 11 node is 70 dB. This is because the distance of CH 1 node to HAP is much closer compared to the distance of CH 11 node to HAP. In addition, the power allocation for the CH 1 node is greater than the CH 11 node.

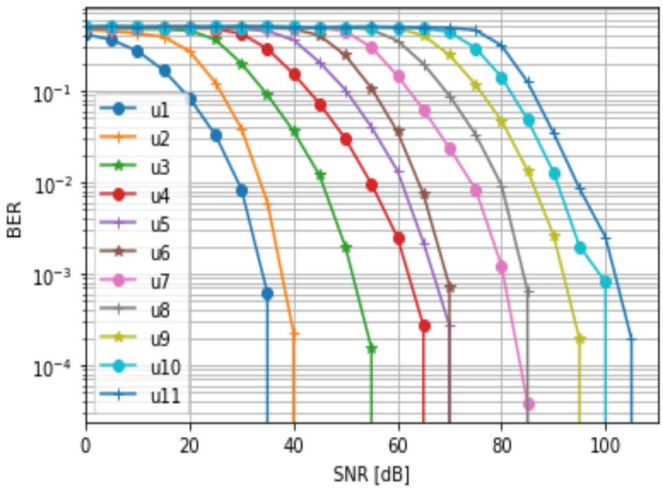

Figure 8. SNR vs BER for HAP moves downwards vertical as far as 4 km by using conventional PD NOMA

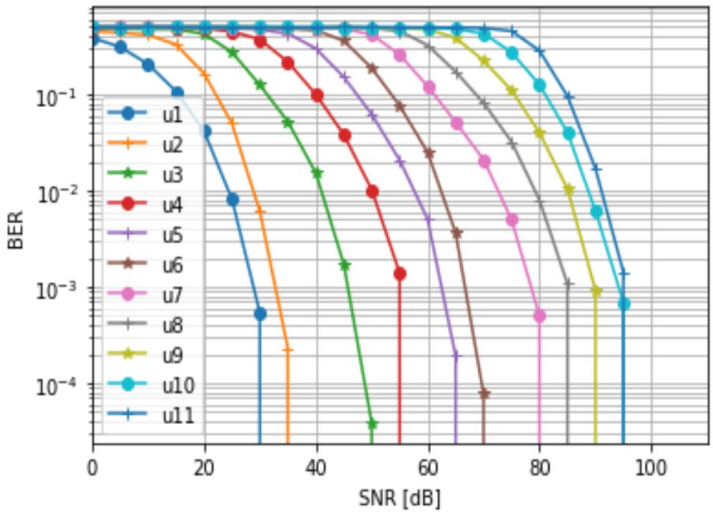

Figure 9. SNR vs BER for HAP moves horizontal rightwards as far as 6.5 km by using conventional PD NOMA

In Figure 9, it can be seen that to reach BER = 10^{-4}, CH 1 (u1) node requires smaller SNR compared to the other CH node, which is 30 dB. The difference in SNR between the CH 1 node and the CH 11 node is 65 dB. This is because the distance of the CH 1 node to HAP is closer compared to the other CH node and also the power allocation for CH 1 node is greater than that of other CH nodes.

In Figure 10, it can be seen that CH 1 (u1) node requires smaller SNR compared to the other CH node, which is 30 dB to reach BER = 10^{-4}. The difference in SNR between the CH 1 node and the CH 11 node is 75 dB. This is because the distance of CH 1 node to HAP is closer compared to the other CH node and also the power allocation for CH 1 node is greater than that of other CH nodes.

From Figures 8, 9, and 10, the CH 1 (u1) node, which is located close to the HAP and has the greatest power allocation, to achieve BER = 10-4 requires a smaller SNR than other CH nodes.

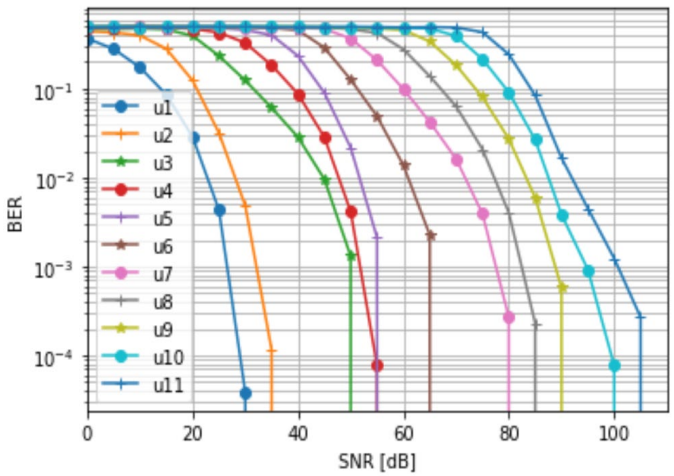

Figure 10. SNR vs BER for HAP moves 10° inclination by using conventional PD NOMA

B. Uplink PD NOMA with CNN

CNN training result for HAP moves horizontal rightwards as far as 6.5 km and can be seen in Figures 11, 12 dan 13.

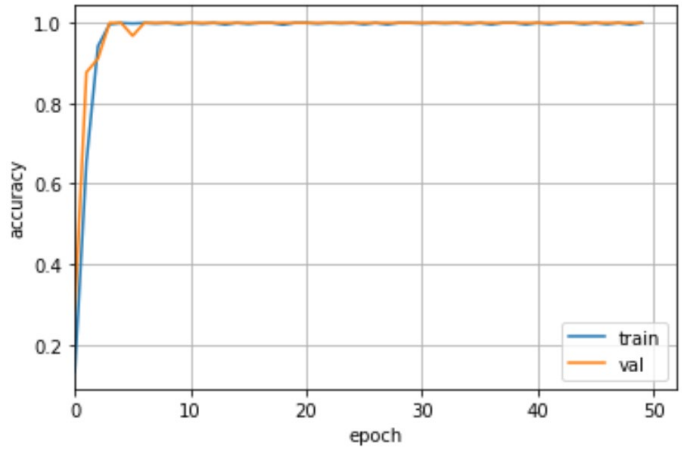

Figure 11. CNN training result for HAP moves vertically as far as 4 km

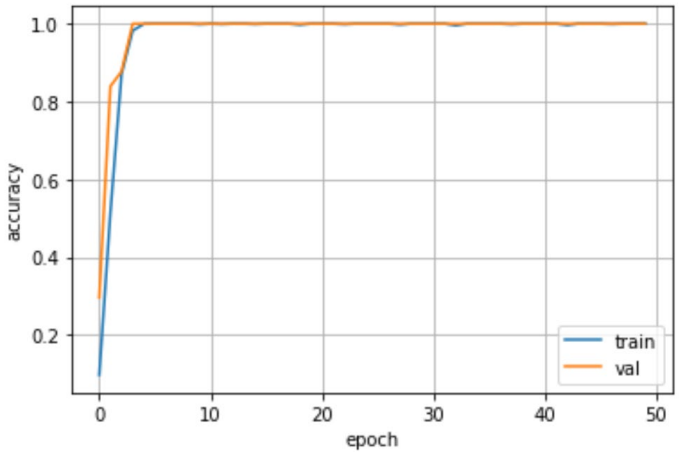

Figure 12. CNN training result for HAP moves horizontal rightwards as far as 6.5 km

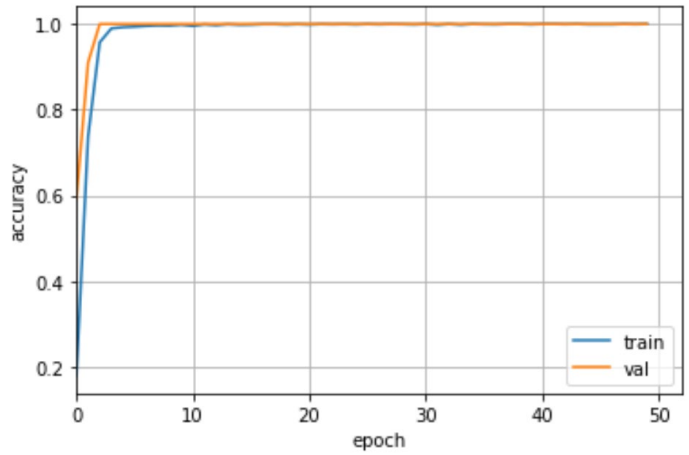

Figure 13. CNN training result for HAP moves 10° inclination

From Figure 11, 12, and 13 it can be seen that to reach 100% accuracy, 50 epoch is required.

The BER simulation results for a HAP-based WSN system using a PD NOMA uplink with CNN as a multiple access technique can be seen in Figures 14, 15, and 16.

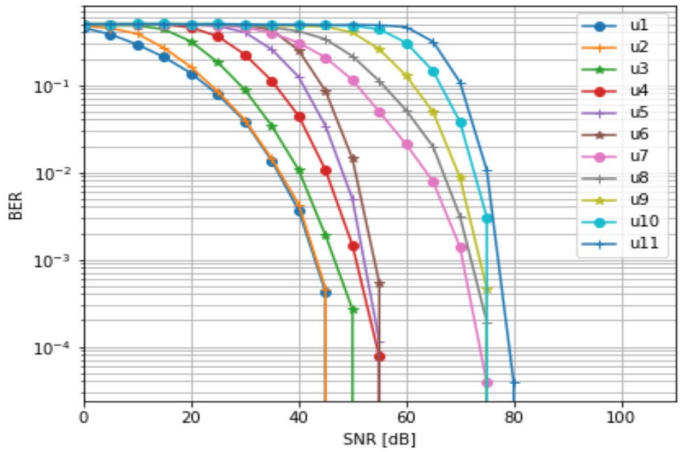

Figure 14. SNR vs BER for HAP moves vertically as far as 4 km by using PD NOMA with CNN

In Figure 14, it can be seen that CH 1 (u1) node require SNR = 45 dB to reach BER = 10^{-4}, whereas CH 11 (u11) node require SNR = 80 dB to reach BER = 10^{-4}. The difference in SNR between the CH 1 node and the CH 11 node is 35 dB. This is because the CH 1 node is located close to the HAP and also has a larger power allocation than the other nodes.

In Figures 8 and 14, it can be seen that the WSN system via HAP using PD NOMA with CNN, requires smaller SNR for CH 3 (u3) node until CH 11 (u11) node compared to the system that uses conventional PD NOMA. However, a system that uses conventional PD NOMA, CH 1 (u1) node, and CH 2 (u2) node requires SNR that is smaller compared to the system that uses PD NOMA with CNN, which is 35 and 40 dB.

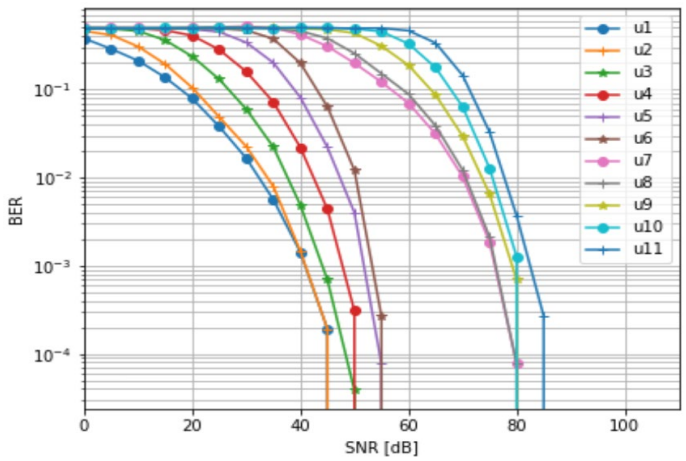

Figure 15. SNR vs BER for HAP moves horizontal rightwards as far as 6.5 km by using PD NOMA with CNN

In Figure 15, it can be seen that to reach BER = 10^{-4}, CH 1 (u1) node require SNR = 45 dB, meanwhile CH 11 (u11) node require SNR = 85 dB. The difference in SNR between the CH 1

node and the CH 11 node is 40 dB. This is because the CH 1 node is located close to the HAP and also has a larger power allocation than the other nodes.

In Figures 9 and 15, it can be seen that the WSN system via HAP that uses PD NOMA with CNN, requires SNR that is smaller for CH 3 (u3) node until CH 11 (u11) node compared to the system that uses conventional PD NOMA. However, the system that uses conventional PD NOMA, CH 1 (u1) node, and CH 2 (u2) node require SNR that is smaller compared to the system that uses PD NOMA with CNN, which is 30 and 35 dB.

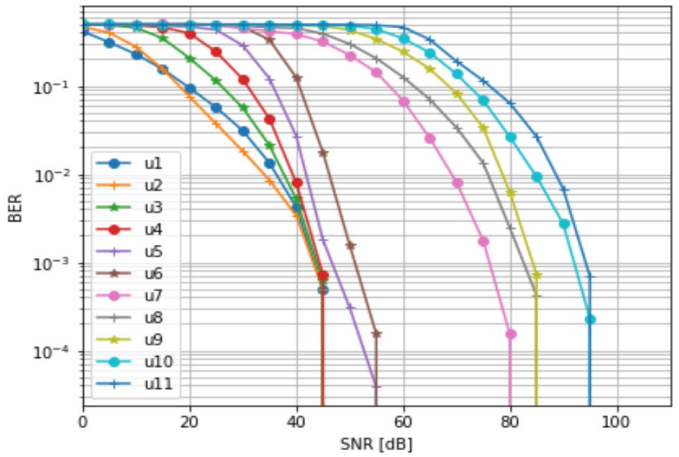

Figure 16. SNR vs BER for HAP moves 10° inclination by using PD NOMA with CNN

From Figure 16, it can be seen that to reach BER = 10^{-4}, CH 1 (u1) node require SNR = 45 dB, meanwhile CH 11 (u11) node require SNR = 95 dB. The difference in SNR between the CH 1 node and the CH 11 node is 50 dB. This is because the CH 1 node is located close to the HAP and also has a larger power allocation than the other nodes.

In Figures 10 and 16, it can be seen that the WSN system via HAP that uses PD NOMA with CNN, requires smaller SNR for CH 3 (u3) node until CH 11 (u11) node compared to the system that uses conventional PD NOMA. However, a system that uses conventional PD NOMA, CH 1 (u1) node, and CH 2 (u2) node require SNR that is smaller than the system that uses PD NOMA with CNN, which is 30 and 35 dB.

From Figures 14, 15, and 16 it can be seen that the CH 1 (u1) node which is located close to the HAP and has the greatest power allocation, to reach BER = 10^{-4} requires a smaller SNR compared to the CH 11 (u11) node which is located far from the HAP.

From Figures 8, 9, 10, 14, 15, and 16, it can be seen that uplink PD NOMA with CNN, to reach BER = 10^{-4}, SNR that is much smaller compared to using conventional uplink PD NOMA is required for 9 CH nodes. Whilst for the CH node that is closer to HAP, which is CH nodes 1(u1) and 2 (u2), to reach BER = 10^{-4}, SNR that is much larger compared to using conventional uplink PD NOMA is required. This is because u1 and u2 have a big power allocation. So that, the detection process in SIC on conventional uplink PD NOMA is easy and the result is better, so to reach BER = 10^{-4}, a smaller SNR than uplink PD NOMA with CNN is required. But if the detection process in SIC for u2 is an error, then u3 will also be an error. And if u3 is an error, then u4 will be an error too, and it continues. This causes conventional uplink PD NOMA, u3 until u11, to reach BER = 10^{-4}, SNR that is greater than uplink PD NOMA with CNN is needed. And this causes the system with conventional uplink PD NOMA requires a larger signal power than a system that uses uplink PD NOMA with CNN to reach BER = 10^{-4}

From Figures 8, 9,10, 14, 15, and 16, it can be seen that conventional uplink PD NOMA suits a system with a little total number of users, which is two users. If the number of users is more than two, then there is more possibility for error interference cancelation to occur. The weakness of the system with convolutional uplink PD NOMA can be overcome by using CNN.

It is seen that uplink PD NOMA with CNN suits a system with a total number of users of more than two.

The tradeoff of the purpose of Replacing the SIC process with CNN is the cost of building and maintaining the machine and the time required for training and testing.

C. Comparison of the complexity of conventional and conventional CNN uplink PD NOMA

The complexity of detection on the conventional uplink PD NOMA which performs the SIC process is as follows:

1. For all iterations *O(I),* where the value of $I \in \{0..\textbf{length}(SNR)\}$ is the number of iterations of SNR trials.
2. For all *O(U)* iterations, where the value of *U* is the largest from several users.
3. The complexity of the SIC calculation (iteratively performed on the user to i+1) is *O(I-1).*
   a. Eliminate the number (-1) because it is not the dominant component in complexity, so it becomes *O(I).*
   b. The complexity of the SIC process on the PD NOMA uplink is as follows:
   *Complexity = O(I)*max(O(U))*
   = O(IU)
4. Because linear iteration and iteration on SPC and SIC are the same, so the complexity becomes:
   Complexity = O(IU)+ O(IU)
   = O(2IU)
   = O(IU)
5. *O(C)* monte carlo iterations are also performed, where C is the largest value of monte carlo.
6. The total complexity of the components for the SIC process on the conventional uplink PD NOMA is as follows:
   *Total Complexity = O(1)*O(IU)* max(C)*
   = O(IUC)

Meanwhile, the complexity of the PD NOMA uplink using CNN is as follows:

1. For all *O(I)* iterations, where the value of $I \in \{0..\textbf{length}(SNR)\}$ is the iteration Number of SNR trials.
2. CNN testing is done the same as the communication system, without doing SIC. The complexity of detection by CNN is iterative from the value *I*. For each value, *I* generate an estimate for 11 users. So, the total complexity of deep learning detection = *O(I).*
3. The iteration of monte carlo *O(C)* is also carried out, where *C* is the largest value of monte carlo
4. The total complexity of the components of the CNN detection process without performing SIC is as follows:
   Total complexity = *O(1)*O(I)*max(C)*
   = O(IC)

From the complexity analysis using Big O Notation, it can be seen that the conventional PD NOMA uplink has a higher complexity than the PD NOMA uplink which uses CNN.

5. Conclusion

From a series of simulations, it can be seen that the CNN implemented on the uplink PD NOMA to replace the conventional SIC can handle NOMA signals without conventional signal processing. Signal processing and detection can be done with CNN.

In both conventional uplink PD NOMA and uplink PD NOMA with CNN, the CH node closest to the HAP required a lower SNR than the CH node farthest from the HAP to achieve BER = 10^{-4}.

In comparison to conventional uplink PD NOMA, CNN provides a smaller SNR difference between CH 1 node and CH 11 node to achieve BER = 10^{-4}, namely 50%, 61.5%, and 66.7% respectively during HAP moving vertically down 4 km, horizontally to the right 6.5 km, and inclination of 10°.

Conventional uplink PD NOMA suits a system with a little total number of users, which is two users. While uplink PD NOMA with CNN suits a system with a total number of users of more than two.

The complexity of uplink PD NOMA using CNN is lower than conventional uplink PD NOMA.

6. References

[1]. L. Dai, B. Wang, Y. Yuan, S. Han, C.-L. I, and Z. Wang, "Non-Orthogonal Multiple Access for 5G: Solutions, Challenges, Opportunities, and Future Research Trends," *IEEE Communications Magazine.*, vol. 53, no. 9, pp. 74–81, September 2015. DOI: 10.1109/MCOM.2015.7263349.

[2]. D. Tze and P. Viswanath, "Fundamentals of Wiress Communication,"Cambridge University Press, New York, 2005.

[3]. L. Dai, B. Wang, Y. Yuan, S. Han, C. Lin and Z. Wang, "Non-Orthogonal Multiple Access for 5G: Solution, Challenges, Opportunities, and Future Research Trends," *IEEE Communications Magazine*, vol. 53, no. 9, pp. 74 – 81, September 2015. DOI: 10.1109/MCOM.2015.7263349.

[4]. S. Verdu, "Multiuser Detection," Cambridge University Press, New York, NY, USA, 1st edition, 1998.

[5]. Z. Yuan, G. Yu and W. Li, "Multi-User Shared Access for 5G," Telecommunication Network Technology, vol. 5, no. 5, pp. 28 – 30, May 2015.

[6]. H. Nikopour and H. Baligh, "Sparse Code Multiple Access," *Proceedings of The IEEE 24th Annual International Symposium on Personal, Indoor, and Mobile Radio Communications (PLMRC'13)*, London, UK, pp. 332 – 336, September 2013.

[7]. R. Hoshyar, F. P. Wathan amd R. Tafazali, "Novel Low-Density Signature for Synchronous CDMA Systems Over AWGN Channel," *IEEE Transactions on Signal Processing*, vol. 50, no. 4, pp. 1616 – 1626, April 2008. DOI: 10.1109/TSP.2007.9093220.

[8]. M. Aldababsa, M. Toka, S. Gokcelim G. K. Kurt and O. Kucur, "A Tutorial on Nonorthogonal Multiple Access for 5G and Beyond," Hindawi Wireless Communication and Mobile Computing, vol. 2018, pp. 1 – 24, June 2018.

[9]. F. A. Rabee, K. Davaslioglu, and R. Gitlin, "The Optimum Received Power Levels of Uplink Nom-Orthogonal Multiple Access (NOMA) Signals," Conference: 2017 IEEE 18th Wireless and Microwave Technology Conference (WAMICON), Cocoa Beach, FL, USA, April 2017. DOI: 10.1109/WAMICON.2017.7930242.

[10]. I. Sim, Y. G. Sun, D. Lee, S. H. Kim, J. Lee, J. H. Kim, Y. Shin and J. Y. Kim, "Deep Learning Based Successive Interference Cancellation Scheme in Nonorthogonal Network Multiple Access Downlink," Energies, vol. 13, no. 23, pp. 1-12, November 2020. DOI:10.3390/en3236237.

[11]. L. Chuan, C. Qing and L. Xianxu, "Uplink NOMA Signal Transmission with Convolutional Neural Networks Approach," Journal of Systems Engineering and Electronics, vol. 31, no. 5, pp. 890-898, November 2020. DOI:10.23919/JSEE.2020.000068.

[12]. M. B. Shahab, S. J. Johnson, M. Shirvanimoghaddam, M. Chafii, E. Basar and M. Dohler, "Index Modulation Aided Uplink NOMA for Massive Machine Type Communications," IEEE Wireless Communications Letters, vol. 9, no. 12, pp. 2159 – 2162, December 2020. DOI: 10.1109/LWC.2020.3015920.

[13]. H. Rajab, F. Benkhelifa and T. Cinkler, "Analysis of Power Allocation for NOMA-Based D2D Communications Using GADIA," Information, vol. 12, no.12, pp. 1 – 24, December 2021.

[14]. V. W. Mahyastuty, Iskandar, Hendrawan and M. S. Arifianto, "Clustering Algorithm for Wireless Sensor Network via High Altitude Platform," *International Journal of Advanced Science and Technology*, vol. 29, no. 08, pp. 1003-1016. 2020.

[15]. Y. Zhang, M. Nekovee, Y. Liu and S. Gjessing, "Cognitive Machine-to-Machine Communications: Visions and Potentials for The Smart Grid," IEEE Network, vol. 26, no. 3, pp. 6-13, May 2012. DOI:10.1109/MNET.2012.6201210.
[16]. Asadi, A., Wang, Q., dan Mancuso, V. (2014): A Survey on Device-to-Device Communication in Cellular Networks, *IEEE Communication Surveys and Tutorials*, 16, 1801-1819.
[17]. M. Agiwal, A. Roy and N. Saxena, "Next Generation 5G Wireless Networks: A Comprehensive Survey," IEEE Communications Surveys and Tutorial, vol. 18, no. 3, pp. 1617-1655, February 2016. DOIl10.1109/COMST.2016.2532458.
[18]. Y. Cao, T. Jiang and Z. Han, "A Survey of Emerging M2M Systems: Context, Task, and Objective," *IEEE Internet of Things Journal*, vol. 3, no. 6, pp. 1246-1258, June 2016. DOI: 10.1109/JIOT.2016.2582540.
[19]. U. Prathap; P. D. Shenoy; K.R. Venugopal; L.M. Patnaik, "Wireless Sensor Networks Applications and Routing Protocols: Survey and Research Challenges," 2012 International Symposium on Cloud and Services Computing, Mangalore, India, pp. 49-56, December 2012. DOI: 10.1109/ISCOS.2012.21.
[20]. I. F. Akyildiz, W. Su, Y. Sankarasubramaniam and E. Cayirci, "A Survey on Sensor Networks," *IEEE Communications Magazine*, vol. 40, no. 8, pp. 102-114, November 2002. DOI: 10.1109/MCOM.2002.1024422.
[21]. D. Grace, C. Spillard, J. Thorntoo and T. C. Tozer, "Channel Assignment Strategies for a High Altitude Platform Spotbeam Architecture," The 13th IEEE International Symposium on Personal, Indoor and Mobile Radio Communications, Lisbon, Portugal, pp. 1586-1590, September 2002. DOI: 10.1109/PIMRC.2002.1045446.
[22]. S. Karapantazis and F. N. Pavlidou, "Broadband Communications via High-Altitude Platforms: A Survey," *IEEE Communications Surveys and Tutorials*, vol. 7, no. 1, pp. 2-31, May 2005. DOI: 10.1109/COMST.2005.1423332.
[23]. B. E. Jabu and R. Steele, "Effect of Positional Instability of an Aerial Platform on Its CDMA Performance," Gateway to 21st Century Communications Village, VTC 1999-Fall, IEEE VTS 50th Vehicular Technology Conference, Amsterdam, Netherlands, pp. 2471-2474, September 1999. DOI: 10.1109/VETECF.1999.800126.
[24]. S.M. R. Islam, N. Avazov, O. A. Dobre and K. S. Kwak, "Power-Domain Non-Orthogonal Multiple Access (NOMA) in 5G Systems: Potentials and Challenges," *IEEE Communications Surveys & Tutorials*," vol. 19, no. 2, pp. 721-742, October 2017. DOI: 10.1109/COMST.2016.2621116.S.
[25]. H. Feng, J. Y. Xu and H. B. Shen, "Artificial Intelligence in Bioinformatics: Automated Methodology Development for Protein Residue Contact Map Prediction," Biomedical Information Technology, 2nd edition, Elsevier Inc, pp. 217-237, 2020. DOI:10.1016/b978-0-12-816034-3.00007-9.
[26]. L. M. Azizah, S. F. Umayah, S. Riyadi, C. Damarjati and N. A. Utama, "Deep Learning Implementation using Convolutional Neural Network in Mangosteen Surface Defect Detection," *2017 7th IEEE International Conference on Control System, Computing and Engineering (ICCSCE)*, pp. 242-246, November 2017. DOI: 10.1109/ICCSCE.2017.8284412.
[27]. Z. Yang, Z. Ding, P. Fan and N. A. Dhahir, "The Impact of Power Allocation on Cooperative Non-orthogonal Multiple Access Networks with SWIPT," *IEEE Transactions on Wireless Communications*, vol. 16, no, 7, pp. 4332 – 4343, May 2017. DOI: 10.1109/TWC.2017.2697380.
[28]. A. Mahmood, S. Khan, S. Hussain and M. Zeeshan, "Performance Analysis of Multi-User Downlink PD-NOMA Under SUI Fading Channel Models," *IEEE Access*, vol. 9, 52851 – 52859, March 2021. DOI: 10.1109/ACCESS.2021.3070147.
[29]. Z. Yang and A. Mohammed, "High Altitude Platforms for Wireless Sensor Network Applications," 2008 *IEEE International Symposium on Wireless Communication*

Systems, Reykjavik, Iceland, 613-617, October 2008. DOI: 10.1109/ISWCS.2008.4726129.
[30]. V. Mathuranathan, "Log Distance Path Loss or Log-Normal Shadowing Model,"https://www.gaussianwaves.com/2013/09/log-distance-path-loss-or-log-normal-shadowing-model/, accessed October. 1, 2019.
[31]. K. K. Talukdar, W. D. Lawing, "Estimation of The Parameters of The Rice Distribution," *The Journal of the Acoustical Society of America*, vol. 89, no. 3, pp. 1193-1197, 1999.
[32]. A. Abdi, C. Tepedelenlioglu, M. Kaveh and G. Giannakis, "On the Estimation of the K Parameter for the Rice Fading Distribution," *IEEE Communications Letters*, vol. 5, no. 3, pp. 92-94, March 2001. DOI: 10.1109/4234.913150.
[33]. Iskandar and S. Shimamoto, "Channel Characterization and Performance Evaluation of Mobile Communication Employing Stratospheric Platform," *IEICE Transactions on Communication*, vol. E89-B, no. 3, pp. 937-944, March 2006.
[34]. Iskandar and S. Shimamoto, "On the Downlink Performance of Stratospheric Platform Mobile Communications Channel" *IEEE Global Telecommunication Conference (Globecom)*, San Francisco, CA, USA, pp. 1-5, 27 November – 1 December 2006. DOI: 10.1109/GLOCOM.2006.922.
[35]. Y. Tang and X. Lan Lv, "Research on The Modulation and Demodulation of BPSK and BDPSK Simulator Based on Matlab," *2011 International Conference on Electrical and Control Engineering*, Yichang, China, pp. 1239-1241, September 2011. DOI: 10.1109/ICECENG.2011.6057217
[36]. Chapter 7: Equalization and Diversity, School of Information Science and Engineering, SDU, http://course.sdu.edu.cn/g2s/ewebeditor/uploadfile/20121213093035437.pdf, accessed April. 29, 2021.

Veronica Windha Mahyastuty received a B.S. in Electrical Engineering from Atma Jaya Catholic University and M.S. degrees in Economics and Business from Gadjah Mada University and Electrical Engineering from ITB in 2001, 2003, and 2007, respectively. Since 2004, she has been a Lecturer at Atma Jaya Catholic University. Now, she is studying as a doctoral student in Electrical Engineering, ITB, Indonesia. Her research interests include routing, medium access control, and wireless communications.

Iskandar completed his B.E. and M.E. degrees in Telecommunication Engineering from Institut Teknologi Bandung (ITB), Indonesia in 1995 and 2000 respectively. He graduated Doctor degree from Waseda University, Japan, in the field of Global Information and Telecommunication Studies (GITS) in 2007. Since April 1997, he has been a permanent lecturer in the electrical engineering department of ITB. His major research interests are in the areas of mobile radio propagation, wireless channel modeling, mobile cellular technology, satellite communication, and high-altitude platform communication.

Hendrawan is lecturesr and researcher at Telematics Laboratory of School of Electrical Engineering and Informatics, Bandung Institute of Technology (ITB), Indonesia. He was received B. Eng in Electrical Engineering from ITB in 1985, MSc. in Telecommunication and Information Systems in 1990, and PhD. In Electronic System Engineering in 1994 both from University of Essex, UK. He is a member of IEEE dan ACM. His research interest includes Telecommunication Performance Engineering, Computer Network and Multimedia.

Mohammad Sigit Arifianto received the B.S. degree in Electrical Engineering from the Institut Teknologi Bandung, Indonesia, in 1998, the M.S. degree in Electrical Engineering from the University at Buffalo, NY, USA, in 2003, and the Ph.D. degree in Telecommunication from the Universiti Malaysia Sabah, Malaysia, in 2010. From 2008 to 2010, he was a lecturer in the Computer Engineering Program of the School of Engineering and Information Technology, the Universiti Malaysia Sabah. In 2010, he joined the School of Electrical Engineering and Informatics, the Institut Teknologi Bandung, in the Telecommunication Engineering Program, where he is currently an Assistant Professor (appointed in 2016). His research interests include the development of new techniques for future wireless communications in the areas of multiple access, multiple-input–multiple-output systems, channel coding, cognitive radio, wireless optical communications, and wireless sensor networks.